PHYSICAL REVIEW D **67**, 091502(R) (2003)

$SU(2)$ Landau gluon propagator on a 140^3 lattice

Attilio Cucchieri* and Tereza Mendes†
Instituto de Física de São Carlos, Universidade de São Paulo, C.P. 369, 13560-970 São Carlos, SP, Brazil

Andre R. Taurines‡
Instituto de Física, Universidade Federal do Rio Grande do Sul, Av. Bento Gonçalves, 9500, Campus do Vale, 91501-970 Porto Alegre, RS, Brazil

(Received 27 February 2003; published 19 May 2003)

We present a numerical study of the gluon propagator in the lattice Landau gauge for three-dimensional pure $SU(2)$ lattice gauge theory at couplings $\beta=4.2$, 5.0, 6.0 and for lattice volumes $V=40^3$, 80^3, 140^3. In the limit of large V we observe a decreasing gluon propagator for momenta smaller than $p_{dec}=350^{+100}_{-50}$ MeV. Data are well fitted by Gribov-like formulas and seem to indicate an infrared critical exponent κ slightly above 0.6, in agreement with recent analytic results.

DOI: 10.1103/PhysRevD.67.091502 PACS number(s): 11.15.Ha, 12.38.Aw, 12.38.Lg, 14.70.Dj

I. INTRODUCTION

The study of the infrared (IR) limit of QCD is of central importance for understanding the mechanism of quark confinement and the dynamics of partons at low energy. Despite being non-gauge-invariant, the gluon propagator is a powerful tool in this (nonperturbative) investigation [1]. In particular, it would be interesting to express it in a closed form for recovering the phenomenology of Pomeron exchange from first principles [2].

Studies of the coupled set of Dyson-Schwinger equations for gluon and ghost propagators in the Landau gauge predict for the gluon propagator an IR behavior of the form $D(p) \sim p^{4\kappa-2}$ [implying $D(0)=0$ if $\kappa>0.5$]. The available predictions for the IR exponent are $\kappa\in[0.52,1.00]$ in the four-dimensional case [3,4] and $\kappa\approx 0.648$ or $\kappa=0.75$ in three dimensions [4].

Furthermore, in the minimal Landau gauge, the gauge-fixed configurations belong to the region Ω of transverse configurations, for which the Faddeev-Popov operator is non-negative. This implies a rigorous inequality [5] for the Fourier components of the gluon field $A_\mu(x)$ and a strong suppression of the gluon propagator in the IR limit. In particular, for dimension d and infinite volume, it is proven that the (unrenormalized) gluon propagator is less singular than p^{2-d} and that, very likely, it vanishes in the IR limit [5]. A vanishing gluon propagator at $p=0$, given by the form $p^2/(p^4+\lambda^4)$, was also obtained by Gribov [6]. Here the mass scale λ arises when the configuration space is restricted to the region Ω. A generalization of this expression has been introduced in Ref. [7] as an ansatz for a nonperturbative solution of the gluon Dyson-Schwinger equation.

Numerical studies [8,9] have now established that the gluon propagator in the lattice Landau gauge shows a turnover in the IR region and attains a finite value for $p=0$. Evidence of a decreasing gluon propagator for small p has been obtained in the 4D $SU(2)$ and $SU(3)$ cases (but only in the strong-coupling regime) [10,11], in the 3D $SU(2)$ case (also in the scaling region) [8,12,13], in the 3D $SU(2)$ adjoint Higgs model [13], in the 4D $SU(2)$ case at finite temperature [14] and for the equal-time three-dimensional transverse gluon propagator in the 4D $SU(2)$ Coulomb gauge [15]. In this last case, one obtains an excellent fit of the transverse propagator by a Gribov-like formula.

This work aims to verify the possibility of using Gribov-like formulas to fit data of the gluon propagator also in Landau gauge. At the same time, we will try to obtain a value for the IR critical exponent κ to be compared to the analytic determinations mentioned above. In order to probe the infinite-volume limit and the IR region we consider the three-dimensional case and the $SU(2)$ group, using lattice sizes up to 140^3. Note that the study of the gluon propagator in three dimensions is also of interest in finite-temperature QCD [16].

II. NUMERICAL SIMULATIONS

We consider the standard Wilson action for $SU(2)$ lattice gauge theory in three dimensions with periodic boundary conditions. The numerical code is entirely parallelized using MPI. (Technical details and a study of the code performance are left for a subsequent work [17].) For the construction of staples we follow Ref. [18]. For the random number generator we use a double-precision implementation of RANLUX (version 2.1) with luxury level set to 2. Computations were performed on the PC cluster at the IFSC-USP. The system has 16 nodes and a server with 866 MHz Pentium III CPU and 256/512 MB RAM memory. The machines are connected with a 100 Mbps full-duplex network. The total computer time used for the runs was about 80 days on the full cluster.

In Table I we report, for each coupling β and lattice volume V, the parameters used for the simulations. All our runs start with a random gauge configuration. For thermalization we use a *hybrid overrelaxed* (HOR) algorithm [19]. Each HOR iteration consists of one heat-bath sweep over the lat-

*Email address: attilio@if.sc.usp.br
†Email address: mendes@if.sc.usp.br
‡Email address: taurines@if.ufrgs.br

TABLE I. The pairs (β,V) considered for the simulations, the number of configurations, the numbers of HOR sweeps used for thermalization and between two consecutive configurations (used for evaluating the gluon propagator) and the parameter p_{sor} used by the SOR algorithm.

β	V	Configurations	Thermalization	Sweeps	p_{sor}
4.2	40^3	400	1100	100	0.70
4.2	80^3	200	2200	200	0.80
4.2	140^3	30	2750	250	0.88
5.0	40^3	400	1320	120	0.69
5.0	80^3	200	2420	220	0.80
5.0	140^3	30	3080	280	0.88
6.0	40^3	400	1540	140	0.68
6.0	80^3	200	2680	240	0.80
6.0	140^3	30	3300	300	0.87

tice followed by m micro-canonical sweeps. We did not try to find the best tuning for m; we use $m=4$ for $V=40^3$, 80^3 and $m=5$ for $V=140^3$. In order to optimize the heat-bath code, we implement two different $SU(2)$ generators, namely methods 1 and 2 described in Ref. [20], Appendix A, with $h_{\rm cutoff}=2$.

For the numerical gauge fixing we use the *stochastic overrelaxation* (SOR) algorithm [21,22] with even/odd update. In Table I we report the value of the tuning parameter p_{sor} used for each pair (β,V). We stop the gauge fixing when the average value of $[(\nabla\cdot A)^b(x)]^2$ is smaller than 10^{-12}. (For a definition of the lattice gauge field $A^b_\mu(x)$ and of the lattice divergence ∇ we refer to [8].) We note that half of the configurations for $V=80^3$ were done using the so-called *Cornell method* [21,22], with tuning parameters $\alpha_{corn}=0.325$, 0.32, 0.316 respectively at $\beta=4.2$, 5.0, 6.0. In fact, the Cornell method is somewhat faster than the SOR algorithm and leads to a gauge fixing of comparable quality if one uses an even/odd update [22]. A good estimator of the quality of the gauge fixing is the quantity Σ_Q [see Eq. (6.8) in Ref. [22]], which should be zero when the configuration is gauge-fixed. By averaging over the gauge-fixed configurations, we find (at $\beta=4.2$) that the ratio between the final and the initial values of Σ_Q is (in 95% of the cases) about 5.3×10^{-10} with the Cornell method and 2.4×10^{-11} with the SOR algorithm. At the same time, the average CPU-time needed for updating each site variable is about 11% smaller for the Cornell method. In any case, the CPU-time for gauge fixing was quite significant for the large lattices. In order to go to even larger lattices one should probably implement a global algorithm such as the Fourier acceleration method [21,22] with the multigrid or conjugate gradient implementations introduced in Ref. [23], which are highly parallelizable.

We ran the 40^3 lattices on a single node, the 80^3 lattices on two nodes and the 140^3 lattices on four nodes. The parallelization of the code worked well. In fact, for runs on 2 and 4 nodes, we obtain speed-up factors 1.82 and 3.41 for the heat-bath link update. For the micro-canonical link update the factors are respectively 1.87 and 3.77 and for the SOR site update we get 1.90 and 3.72.

TABLE II. For each coupling β we report the value of the average plaquette $\langle W_{1,1}\rangle$, the string tension $\sqrt{\sigma}$ in lattice units, the lattice spacing in fm and the smallest nonzero momentum (in MeV) for the lattice volume $V=140^3$. Error bars for $\langle W_{1,1}\rangle$ have been obtained taking into account the integrated autocorrelation time of the HOR algorithm. All the other error bars come from propagation of errors.

β	$\langle W_{1,1}\rangle$	$\sqrt{\sigma}$	a (fm)	$p_{\rm min}$ (MeV)
4.2	0.741861(2)	0.387(3)	0.174(1)	59.0(4)
5.0	0.786869(2)	0.314(2)	0.1407(8)	62.9(4)
6.0	0.824780(1)	0.254(1)	0.1138(5)	77.8(4)

For each β we evaluate the average plaquette $\langle W_{1,1}\rangle$ (see Table II). Results are in agreement with the data reported in Ref. [8], but we now have smaller statistical errors. (The data have been analyzed using various methods, described in footnote 4 of Ref. [8]. Here we always report the largest error found.) We also evaluate the tadpole-improved coupling $\beta_I\equiv\beta\langle W_{1,1}\rangle$. In this way, by using the fit given in Eq. (2) and Table IV of Ref. [24] we calculate the string tension $\sqrt{\sigma}$ in lattice units (see Table II) and the inverse lattice spacing a^{-1} using the input value $\sqrt{\sigma}=0.44$ GeV. The fit is valid for $\beta\gtrsim3.0$, i.e. the couplings β considered here are well above the strong-coupling region. Let us notice that, if we compare the data for the string tension (in lattice units) with data obtained for the $SU(2)$ group in four dimensions [[25], Table 3], then our values of β correspond to $\beta\approx2.28$, 2.345, 2.41 in the four dimensional case. Finally, in the same table we report the lattice spacing a in fm and the smallest nonzero momentum (in MeV) that can be considered for each β. Thus, with the lattice volumes and the β values used here we are able to consider momenta as small as 59 MeV (in the deep IR region) and physical lattice sides almost as large as 25 fm.

In this work we did not do a systematic study of Gribov-copy effects for the gluon propagator. However, we compared data obtained using the SOR and the Cornell gauge-fixing methods. In principle, different gauge-fixing algorithms—or even the same algorithm with different values of the tuning parameter [26]—can generate different Gribov copies starting from the same thermalized configuration. Thus, this comparison provides an estimate of the bias (Gribov noise) introduced by the gauge-fixing procedure. We found that, in most cases, the difference between the two sets of gluon-propagator data is within 1 standard deviation and that, in all cases, it is smaller than 2 standard deviations. Moreover, this difference did not show any systematic effect, suggesting that the influence of Gribov copies on the gluon propagator (if present) is of the order of magnitude of the numerical accuracy. This is in agreement with previous studies in Landau gauge for the $SU(2)$ and $SU(3)$ groups in four dimensions [10,26,27]. A similar result has also been obtained for the Coulomb gauge [28]. Note that, in the $U(1)$ case [29], Gribov copies can affect the behavior of the photon propagator, making it difficult to reproduce the known perturbative behavior in the Coulomb phase. The situation is very different for the $SU(2)$ and $SU(3)$ cases, at least when considering the lattice Landau gauge. In fact, as said in the

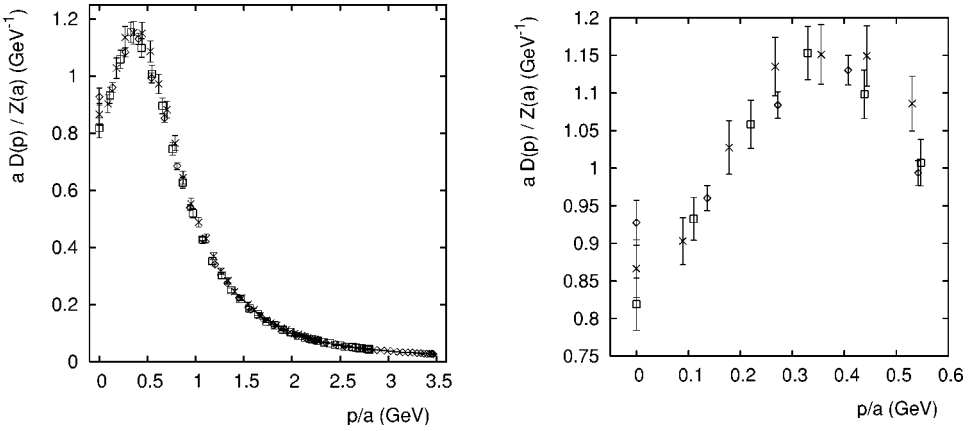

FIG. 1. Plot of the rescaled gluon propagator as a function of the lattice momentum for $V=80^3$ and $\beta=4.2$ (×), 5.0 (□), 6.0 (◇). The second plot shows only the IR region. Error bars are obtained from propagation of errors.

Introduction, in the non-Abelian case the minimal-Landau-gauge condition implies [5] the positiveness of the Faddeev-Popov matrix and a strict bound for the Fourier components of the gluon field $A_\mu(k)$. The bound applies to all Gribov copies obtained with the numerical gauge fixing. Thus, if the behavior of the gluon propagator is determined by this bound [5,6], then this behavior should be the same for all lattice Gribov copies. This would explain why we do not see Gribov-copy effects here. Clearly, the same result does not apply to the $U(1)$ theory, since in this case the Faddeev-Popov matrix is independent of the gauge field.

III. RESULTS AND CONCLUSIONS

We evaluate the lattice gluon propagator $D(k)$ and study it as a function of the lattice momentum $p^2(k)$ (see Ref. [8] for definitions). In our simulations we consider, for each gauge-fixed configuration, all vectors $k\equiv(k_x,k_y,k_t)$ with only one component different from zero and average over the three directions. For the gluon propagator we analyze the data by estimating the statistical error with three different methods: standard deviation, jack-knife with single-data elimination and bootstrap (with 10000 samples). We found that the results obtained are in agreement in all cases. Here we always use the standard-deviation error.

Let us recall that in the three-dimensional case the coupling g^2 has dimensions of mass. Thus, in order to obtain a dimensionless lattice coupling we have to set $\beta=4/(ag^2)$. Then, with our notation [8], the quantity $aD(k)$ approaches $g^2D^{(cont)}(k)/4$ in the continuum limit, where $D^{(cont)}(k)$ is the unrenormalized continuum gluon propagator.

In order to compare lattice data at different β's, we apply the matching technique described in [[30], Sec. V B 2]. (Note that we have already determined the lattice spacing a, as described above.) We start by checking for finite-size effects, comparing data at different lattice sizes and same β value. In this way, we find (for each β) a range of ultraviolet (UV) momenta for which the data are free from finite-volume corrections. We then perform the matching using data for these momenta and $V=40^3$, since for this lattice volume the errors are smallest (about 1%). In particular, when matching data obtained at two different values of β, we first interpolate the data for the larger β (the fine lattice) using a spline. Finally, we find the multiplicative factor $R_Z=Z(a_f)/Z(a_c)$ corresponding to the best fit of the (multiplied) coarse-lattice data to the same spline. The error of R_Z is estimated using a procedure similar to the one described in [30]. The method works very well (see Fig. 1). Notice that we did not fix the remaining global factor Z imposing a renormalization condition, as done for example in Ref. [31]. Our case is equivalent to setting $Z(a)=1$ at $\beta=6.0$.

The data obtained after the matching are shown for $V=80^3$ in Fig. 1. Clearly, we find that the gluon propagator decreases in the IR limit for momenta smaller than p_{dec}, which corresponds to the mass scale λ in a Gribov-like propagator. From the plot we can estimate $p_{dec}=350^{+100}_{-50}$ MeV, in agreement with Ref. [8].

In Fig. 2 we plot the rescaled gluon propagator at zero momentum, namely $aD(0)/Z(a)$, as a function of the inverse lattice side $L^{-1}=1/(aN)$ in physical units (fm^{-1}). We see that $aD(0)/Z(a)$ decreases monotonically as L increases, in agreement with Ref. [9]. It is interesting to notice that these data can be well fitted using the simple ansatz $d+b/L^c$ both with $d=0$ and $d\neq0$ (see Fig. 2). In order to decide for one or the other result one should go to significantly larger lattice sizes. We plan [32] to extend these simulations to $\beta=3.4$ and lattice sizes up to 260^3, allowing us to

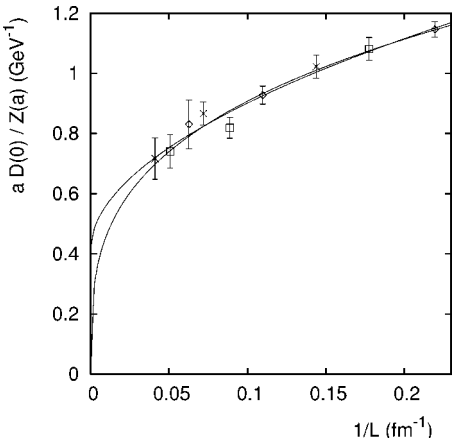

FIG. 2. Plot of the rescaled gluon propagator at zero momentum as a function of the inverse lattice side for $\beta=4.2$ (×), 5.0 (□), 6.0 (◇). We also show the fit of the data using the ansatz $d+b/L^c$ both with $d=0$ and $d\neq0$. Error bars are obtained from propagation of errors.

TABLE III. Fit of the data using Eqs. (1) and (2). In all cases χ^2/DBF was of order 1. Note that for a lattice volume $V=N^3$ we have $1+N/2$ data points and that all points have been used for the fits.

		Fit 1			Fit 2	
β	V	α	x	$\lvert y\rvert$	α	y^2
4.2	40^3	0.69(2)	0.17(2)	0.42(1)	0.48(4)	0.29(1)
4.2	80^3	0.66(2)	0.17(2)	0.36(1)	0.46(4)	0.24(1)
4.2	140^3	0.61(4)	0.19(4)	0.35(3)	0.38(6)	0.25(2)
5.0	40^3	0.77(3)	0.11(2)	0.28(2)	0.53(6)	0.152(8)
5.0	80^3	0.71(2)	0.11(1)	0.214(9)	0.45(3)	0.118(6)
5.0	140^3	0.71(3)	0.10(2)	0.22(2)	0.44(6)	0.12(1)
6.0	40^3	0.86(3)	0.069(8)	0.20(2)	0.64(6)	0.082(6)
6.0	80^3	0.84(2)	0.032(6)	0.166(8)	0.65(5)	0.051(3)
6.0	140^3	0.80(2)	0.037(8)	0.123(7)	0.55(6)	0.040(4)

consider a value $L^{-1}\approx 0.017$ fm^{-1}. (This requires running in parallel on all nodes of our PC cluster.)

Following Ref. [15] we fit the data using a Gribov-like (or Stingl-like) formula

$$D(p)=\frac{s+zp^{2\alpha}}{y^2+(p^2+x)^2}, \tag{1}$$

where z, s, α, x and y are fitting parameters. For non-negative α this implies a finite gluon propagator in the IR limit, with a behavior given by $D(p)\propto(s+zp^{2\alpha})$. If $y^2>0$ this form corresponds to a propagator with poles at $m_{\pm}^2=-x\pm iy$, while if $y^2\leqslant 0$ the poles are real. Finally, note that the IR exponent κ considered in studies of Dyson-Schwinger equations is given in terms of α by $\kappa=(1+\alpha)/2$, assuming $D(0)=0$. Results of our fits using the un-rescaled lattice data $D(k)$ are reported in Table III. We see that α decreases when the physical lattice volume increases. Also, we always get $y^2>0$ and $x<|y|$, which seems to support the scenario of purely imaginary poles found in [15]. Let us recall that the poles of the gluon propagator are gauge-invariant (at all orders in perturbation theory) [33].

Notice that this fitting form leads in general to the wrong UV behavior, namely $D(p)\sim p^{2\alpha-4}$. This is not a serious problem, since the largest momentum we can consider is about 3.5 GeV, i.e. we are not really exploring the UV limit. On the other hand, the exponent α in Eq. (1) plays a role both in the IR and in the UV regimes. Thus, the values obtained for α probably correspond to averaging the behavior of the gluon propagator in these two regions. In particular, since we expect $D(p)\sim p^{-2}$ in the UV limit, it is likely that the IR behavior of the propagator be given by a smaller exponent α than the ones reported in Table III. To check this we set $x=0$ and introduce an anomalous dimension γ:

$$D(p)=\frac{s+zp^{2\alpha}}{y^2+p^{2(1+\gamma)}}. \tag{2}$$

Results for this fitting form are also reported in Table III. Indeed, we get values of α smaller than in the previous case (and still decreasing with increasing physical lattice volume). For the anomalous dimension we obtain $\gamma\approx 0.65$, with small volume and β dependence. The problem with Eq. (2) is that the introduction of γ compromises the pole interpretation.

Finally, one can also try the form

$$D(p)=\frac{s+zp^{2\alpha}}{(y^2+p^4)^{\gamma}}. \tag{3}$$

This corresponds to a propagator with purely imaginary poles $m_{\pm}^2=\pm iy$ and at the same time allows the data to select the IR and the UV behaviors separately. The problem in this case is that the fit is unstable for small lattice volumes. On the contrary, for $V=140^3$ the fit works well and we obtain $\alpha=0.27(6)$, 0.29(7), 0.38(8) respectively for $\beta=4.2$, 5.0, 6.0 and $\gamma\approx 0.72$. Hence, our α values are of the order of 0.3, corresponding to $\kappa\approx 0.65$. (Again, there is a decrease of α when the physical lattice volume increases.)

In order to check for possible effects from the breaking of rotational invariance [34] we redid our fits substituting $p^2(k)$ by $\tilde{p}^2(k)\equiv p^2(k)+p^{[4]}(k)/12$ (see Ref. [35]). One expects this modification to play an important role in the UV limit and to have a small effect in the IR case. For all β values and lattice volumes we obtain good fits and results similar to those reported above. In particular, using Eq. (1) one still finds $y^2>0$ and $x<|y|$, supporting the scenario of purely imaginary poles. At the same time, for the three fitting functions, α decreases when the physical lattice volume increases, but its value is about 20–30% larger than the one reported in Table III and above. In particular, using Eq. (3) and data for $V=140^3$ we obtain $\alpha=0.32(7)$, 0.39(8), 0.59(12) respectively for $\beta=4.2$, 5.0, 6.0 and $\gamma\approx 0.7$. This implies slightly larger values for $\kappa=(1+\alpha)/2$. The analysis of these discretization effects and their influence on the extrapolation of α and κ to the continuum limit will be done elsewhere [32].

We have confirmed, by numerical simulations in the scaling region, that the transverse gluon propagator in 3D $SU(2)$ Landau gauge is a decreasing function for momenta $p\lesssim 350$ MeV (attaining a finite value at $p=0$). Also, the data are well fitted by the Gribov-like formulas (1)–(3) and we obtain an IR critical exponent κ in agreement with recent analytic results. In order to eliminate remaining discretization and finite-volume effects [and in particular to check if $D(0)=0$], we need to simulate at larger lattice volumes and at other values of β.

ACKNOWLEDGMENTS

We thank Reinhard Alkofer, Terry Goldman, Kurt Langfeld, Axel Maas and Dan Zwanziger for helpful comments and suggestions and Martin Lüscher for sending us the latest double-precision version of the RANLUX random number generator. The research of A.C. and T.M. is supported by FAPESP (Project No. 00/05047-5). A.T. thanks CNPq for financial support and the IFSC-USP for hospitality.

[1] See, for example, C. D. Roberts, nucl-th/9807026; R. Alkofer and L. von Smekal, Phys. Rep. **353**, 281 (2001).
[2] F. Halzen, G. I. Krein, and A. A. Natale, Phys. Rev. D **47**, 295 (1993); M. B. Gay Ducati, F. Halzen, and A. A. Natale, *ibid.* **48**, 2324 (1993).
[3] L. von Smekal, R. Alkofer, and A. Hauck, Phys. Rev. Lett. **79**, 3591 (1997); D. Atkinson and J. C. R. Bloch, Phys. Rev. D **58**, 094036 (1998); Mod. Phys. Lett. A **13**, 1055 (1998); C. Lerche and L. von Smekal, Phys. Rev. D **65**, 125006 (2002); C. S. Fischer, R. Alkofer, and H. Reinhardt, *ibid.* **65**, 094008 (2002); D. Zwanziger, **67**, 105001 (2003).
[4] D. Zwanziger, Phys. Rev. D **65**, 094039 (2002).
[5] D. Zwanziger, Phys. Lett. B **257**, 168 (1991); Nucl. Phys. **B364**, 127 (1991); **B412**, 657 (1994).
[6] V. N. Gribov, Nucl. Phys. **B139**, 1 (1978).
[7] M. Stingl, Phys. Rev. D **34**, 3863 (1986); **36**, 651(E) (1987).
[8] A. Cucchieri, Phys. Rev. D **60**, 034508 (1999).
[9] F. D. Bonnet *et al.*, Phys. Rev. D **64**, 034501 (2001).
[10] A. Cucchieri, Nucl. Phys. **B508**, 353 (1997).
[11] A. Cucchieri, Phys. Lett. B **422**, 233 (1998); H. Nakajima and S. Furui, Nucl. Phys. B (Proc. Suppl.) **73**, 635 (1999).
[12] A. Cucchieri, F. Karsch, and P. Petreczky, Phys. Lett. B **497**, 80 (2001).
[13] A. Cucchieri, F. Karsch, and P. Petreczky, Phys. Rev. D **64**, 036001 (2001).
[14] I. L. Bogolubsky and V. K. Mitrijushkin, hep-lat/0204006.
[15] A. Cucchieri and D. Zwanziger, Phys. Lett. B **524**, 123 (2002).
[16] F. Karsch, M. Oevers, and P. Petreczky, Phys. Lett. B **442**, 291 (1998); A. Maas *et al.*, hep-ph/0210178.
[17] A. Cucchieri, T. Mendes, A. Taurines, and G. Travieso (in preparation).
[18] S. Hioki, Parallel Comput. **22**, 1335 (1997).
[19] F. R. Brown and T. J. Woch, Phys. Rev. Lett. **58**, 2394 (1987); U. Wolff, Phys. Lett. B **288**, 166 (1992).
[20] R. G. Edwards *et al.*, Nucl. Phys. **B380**, 621 (1992).
[21] A. Cucchieri and T. Mendes, Nucl. Phys. **B471**, 263 (1996); Nucl. Phys. B (Proc. Suppl.) **53**, 811 (1997).
[22] A. Cucchieri and T. Mendes, hep-lat/0301019.
[23] A. Cucchieri and T. Mendes, Phys. Rev. D **57**, 3822 (1998).
[24] B. Lucini and M. Teper, Phys. Rev. D **66**, 097502 (2002).
[25] J. Fingberg, U. M. Heller, and F. Karsch, Nucl. Phys. **B392**, 493 (1993).
[26] L. Giusti *et al.*, Int. J. Mod. Phys. A **16**, 3487 (2001).
[27] J. E. Mandula, Phys. Rep. **315**, 273 (1999).
[28] A. Cucchieri and D. Zwanziger, Phys. Rev. D **65**, 014001 (2002).
[29] A. Nakamura and M. Plewnia, Phys. Lett. B **255**, 274 (1991); S. Durr and P. de Forcrand, Phys. Rev. D **66**, 094504 (2002).
[30] D. B. Leinweber *et al.*, Phys. Rev. D **60**, 094507 (1999); **61**, 079901(E) (2000).
[31] C. Alexandrou, P. de Forcrand, and E. Follana, Phys. Rev. D **65**, 117502 (2002).
[32] A. Cucchieri, T. Mendes, and A. Taurines (in preparation).
[33] N. K. Nielsen, Nucl. Phys. **B101**, 173 (1975); R. Kobes, G. Kunstatter, and A. Rebhan, Phys. Rev. Lett. **64**, 2992 (1990).
[34] D. Becirevic *et al.*, Phys. Rev. D **60**, 094509 (1999).
[35] J. P. Ma, Mod. Phys. Lett. A **15**, 229 (2000).